Review

Opaque Coloured Building Integrated Photovoltaic (BIPV): A Review of Models and Simulation Frameworks for Performance Optimisation

Martina Pelle [1,2] ![ORCID], **Francesco Causone** [2,*] ![ORCID], **Laura Maturi** [1] **and David Moser** [1] ![ORCID]

1   Institute for Renewable Energy, Eurac Research, 29100 Bolzano, Italy
2   Department of Energy, Politecnico di Milano, Via Lambruschini 4, 20156 Milano, Italy
*   Correspondence: francesco.causone@polimi.it

Abstract: Coloured building integrated photovoltaics (BIPVs) may contribute to meeting the decarbonisation targets of European and other countries. Nevertheless, their market uptake has been hindered by a lack of social acceptance, technical issues, and low economic profitability. Being able to assess in advance the influence of the coloured layers on a module's power generation may help reduce the need for prototyping, thereby allowing optimisation of the product performance by reducing the time and costs of customised manufacturing. Therefore, this review aims at investigating the available literature on models and techniques used for assessing the influence of coloured layers on power generation in customised BIPV products. Existing models in the literature use two main approaches: (i) detailed optical modelling of the layers in the module's stack, including coloured layers, and (ii) mathematical elaboration of the final product's measured characteristics. Combining the two approaches can provide improved future models, which can accurately assess every single layer in the module's stack starting from measured parameters obtained with simpler equipment and procedures.

Keywords: coloured BIPV; optimization; simulation

1. Introduction

Building integrated photovoltaics (BIPVs) constitutes a solution to the problem of incorporating renewable energy sources (RESs) into the built environment by using photovoltaic technologies as a construction material and as a power generation system at the same time. The twofold purpose of this technology can unlock the solar potential of a large set of vertical and horizontal envelope surfaces typically not exploited, harvesting solar energy for on-site energy production and leading the building stock to energy flexibility and self-sufficiency [1,2]. These aspects are particularly relevant in densely built environments since they promote equal access to renewable energy production for users living in urban areas, where several constraints hinder the exploitation of solar energy, i.e., where traditional ground-mounted photovoltaic (PV) installations are not possible and the solar potential for roof-mounted PVs is low compared to the multi-property and multi-story-building energy demand [3–5]. Furthermore, exploiting building surfaces for solar energy harvesting can contribute to meeting the targets for renewable energy penetration in a country's energy mix (as in the case of European member states), while reducing the need for the allocation of land to solar farms [6]. Recent studies have highlighted that reaching the complete decarbonisation of the Italian electricity system by 2030, while also guaranteeing national power self-sufficiency at minimum costs, would require the installation of about 200 GW of solar power, which equates to approximately 1200 km^2 of installed PV modules [7]. Building integrated photovoltaics have the potential to contribute considerably to the installation of such solar power, but the market uptake of these technologies has faced some major hurdles, namely, social acceptance, technical issues, and low economic profitability, which

have been due to aesthetic issues, low power conversion efficiency, and high costs [8–11]. In the last few years, the BIPV industry has addressed quite effectively the first two aspects, by improving on the one hand the aesthetic quality and the uniformity of BIPV installations, using appropriate mounting structures to integrate the PV panels in the envelope, and on the other hand by introducing coloured products to overcome the typical narrow aesthetic variability of the standard PV modules [3,12], sometimes considered by users and architects as unsuitable and incoherent with urban contexts [13,14]. Therefore, broader architectural application claims for enhancements in the visual rendering of BIPV modules [11], and the development of modules that can disguise the PV cells beneath coloured patterns, thereby limiting the perception of the actual material of the cells, have improved the aesthetic acceptability of BIPV applications. In particular, the modules' aesthetic has been improved by hindering or modifying the perception of the original material of the PV cells through coloured layers that make the modules' appearance comparable to standard construction products; however, the introduction of coloured layers goes to the detriment of the final module's efficiency [15–17] and leads to an increase in costs [18]. Indeed, to display colours, a portion of the solar radiation in the visible spectrum is reflected from the modules' surface to the user's eyes, thus being subtracted from the power conversion [16,17,19]. The increase in costs is due to (i) the increase in manufacturing costs due to the introduction of coloured features or layers, which modify the standard manufacturing process of an uncoloured product; and (ii) the reduction of the energy yield of the BIPV system, which affects the economic profitability of the installation [20]. The higher manufacturing cost depends strongly on the required customisation. Indeed, besides the material costs, customising a product for a specific purpose would imply the manufacturing of several samples to reach the desired aesthetic effect, while the electric performance is evaluated by testing the finished product [21]. Being able to assess in advance the influence of the coloured layers on the module's power generation, would, on the contrary, reduce the need for prototyping, thereby allowing optimisation of the product performance by reducing the time and costs of customised manufacturing [20,22].

In the last few years, some research has investigated the manufacturing process of coloured PV modules, and different technologies have been demonstrated. Furthermore, experimental evaluations of the electric behaviour of coloured modules have been conducted, including in real exposure conditions [23–28], and reviews have been published about the available technologies and their related performance [6,14,29–31]. On the other hand, the scientific literature is currently lacking an extensive review of the models and simulation frameworks used to assess and investigate the relation between colours and performance in BIPVs. Therefore, this review aims at investigating extensively the available literature on models and techniques used for assessing the influence of coloured layers on power generation in customised opaque BIPV products, which are the most suitable for being installed on façades and roofs to meet the solar power installation target. Predicting the impact of coloured layers on a module's power generation is considered a key step in helping to reduce the cost of coloured BIPV products, by easing mass manufacturing while preserving the customisation potential and, therefore, enhancing the market uptake of this technology in the construction sector [22,32]. In the following section, the methodology of this study is described first. Then, an overview of existing technologies for coloured BIPVs is provided, and the results of a detailed and critical literature analysis of the existing models and simulation frameworks for linking aesthetic and energy features in opaque coloured BIPVs are presented. In the conclusion, we discuss the future challenges to be addressed in the development of more accurate models.

2. Methods

A systematic review has been conducted by interrogating bibliometric databases (Scopus, Web of Science, Google Scholar) and using the keywords "BIPV" OR "building integrated photovoltaics" AND "color" OR "colour" to be found in the title, abstract, or keywords of the analysed studies. The review structure is schematized in Figure 1. The

search resulted in the identification of over 200 published papers, which have undergone a further filtering process through detailed analysis of the abstracts. The filtering aimed at selecting only the studies which presented (i) simulations to determine the final colour and the related electric performance of an opaque BIPV device, or (ii) mathematical modelling or methodologies for fine-tuning the colour properties of opaque BIPV devices to optimise their electric performance. From the screening of the abstracts, all the papers dealing with the simulation or optimisation of neutral colour or semi-transparent BIPV products were excluded, since these papers investigate mainly the colour rendering index (CRI) [33] of semi-transparent BIPVs, for which the display of any colours is undesirable.
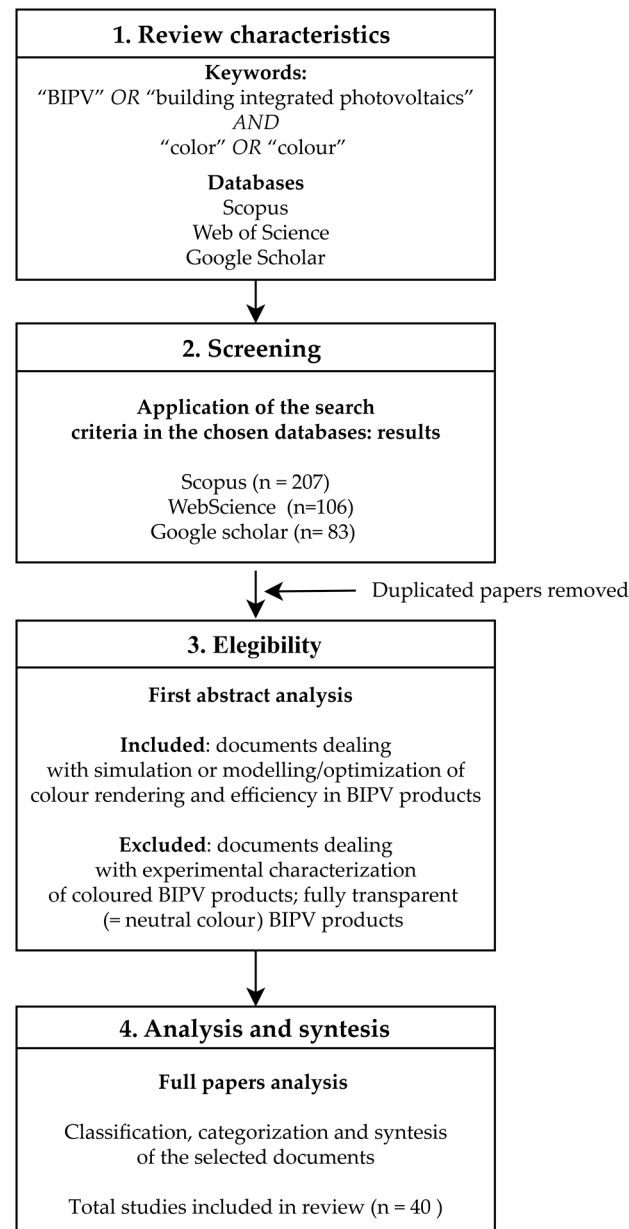
1. Review characteristics

Keywords:
"BIPV" *OR* "building integrated photovoltaics"
AND
"color" *OR* "colour"

Databases
Scopus
Web of Science
Google Scholar

2. Screening

**Application of the search
criteria in the chosen databases: results**

Scopus (n = 207)
WebScience (n=106)
Google scholar (n= 83)

Duplicated papers removed

3. Elegibility

First abstract analysis

Included: documents dealing
with simulation or modelling/optimization of
colour rendering and efficiency in BIPV products

Excluded: documents dealing
with experimental characterization
of coloured BIPV products; fully transparent
(= neutral colour) BIPV products

4. Analysis and syntesis

Full papers analysis

Classification, categorization and syntesis
of the selected documents

Total studies included in review (n = 40)

Figure 1. Review approach and structure.

3. Overview of the Existing Techniques to Apply Colour in BIPV Modules

For modules currently available on the market, various customisation approaches are employed to apply colours or textures. These approaches can be categorised into two main groups, according to the position of the coloured element in relation to the active layer of the module stack: coloured layers can be (i) added to the module assembly, behind or in

front of the active layers, or (ii) integrated as an inherent part of the active layer [34]. The addition of a coloured layer beneath the PV module's active components has no impact on how efficiently solar radiation is converted into electricity, and as a result, the system's energy production is unaffected (Figure 2e). On the other hand, when coloured layers are placed between the active layer and the light source, or when they are integrated within the active layer, they change the spectral power distribution of the solar radiation available for power conversion, because some of it is reflected in the visible spectrum to display colours [16,17,19]. The integration of colours in the active layer of BIPV technologies implies that the colouring features are introduced in the manufacturing process of the PV cells, within the active layers (Figure 2d). This means that the colour is coherent with the PV material and cannot be separated from it. This can be done by including different dyes in the production of perovskite solar cells, dye-sensitised solar cells (DSSCs), colloidal quantum dot solar cells (CQD PVs), or employing active materials that exhibit different absorption spectra in semi-transparent organic photovoltaic cells (OPVs) [35]. The appearance of the modules produced with such a technique is uniform, translucent, and coloured. When it comes to opaque photovoltaics that use crystalline silicon (c-Si) or CIGS PV cells [36–38], the colour is introduced by modifying the thickness and the refractive index of the passivation or anti-reflection coating (ARC) of the cell. The appearance of the modules produced with such a technique is usually iridescent and can present different colours according to the typology and thickness of the coating. Adding a coloured layer between the active layer and the light source implies that, during the lamination process, an extra layer is added to the module stack. According to the architectural requirements, the coloured layer can be inserted into an interlayer or encapsulant film (Figure 2a), or by modifying the front glass (Figure 2b,c) by printing, coating, wrapped polymeric films, or texturing. The appearance of the modules produced with such techniques presents high customisation potential since every added layer can appear either uniform or translucent, or present high-definition images or patterns that can be obtained by digital printing [3,23,31]. Another advantage of adding layers is that they can be applied to several BIPV technologies, including crystalline and amorphous silicon, thin-film, and perovskite, without interfering with the manufacturing of the active components. Table 1 summarises the existing colouring techniques and the technology to which they can be applied, highlighting the position of the coloured layer in the module stack and its main features.
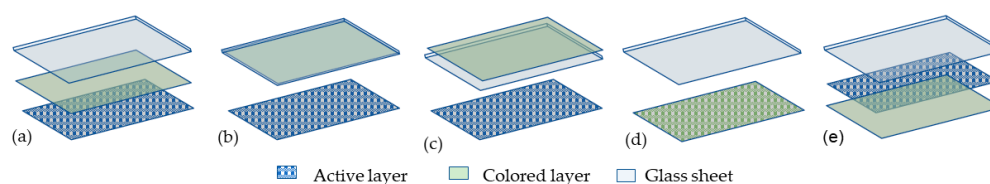

Figure 2. Relative position of the coloured layer in the BIPV module assembly: (**a**) coloured interlayer or encapsulant; (**b**) coloured coated front glass; (**c**) coloured layer on top of the front glass; (**d**) coloured or coated active layer; (**e**) coloured back sheet.

Table 1. Existing colouring technique for modulating the aesthetic of BIPV modules.

Coloured Layer Position	Colouring Technique	Technology	Colour Layer Typology
Integrated (or embedded)	Dyes addition	OPV Perovskite DSSC	Continuous
	Modification in the chemical composition of the active layer	OPV Perovskite	Continuous
	Modulation of the passivation coating or ARC thickness and/or refraction index	c-SI CIGS	Continuous

Table 1. *Cont.*

Coloured Layer Position	Colouring Technique	Technology	Colour Layer Typology
Added (additional layer)	Ceramic printing of the front glass	c-SI CIGS Perovskite	Continuous/discrete
	Printing of encapsulant material	c-SI OPV	Continuous/discrete
	Additional coloured/printed interlayer	c-SI CIGS Perovskite LSC	Continuous/discrete

4. Influence of Colour on BIPV Power Output

4.1. Human Colour Perception

Colours are the elaboration of the human brain of the stimuli provided by the human visual system receptors, called cones, when a certain spectral distribution of light is impinging on them [39]. Colourimetry is the science that aims at quantifying and describing human colour perception, by correlating the power distribution of the electromagnetic spectrum in the visible range and the colours physiologically perceived by human vision [40]. These models use standardised responses of the human eye, the colour matching functions, $\overline{x}(\lambda)$, $\overline{y}(\lambda)$, and $\overline{z}(\lambda)$ (Figure 3), that describe the spectral sensitivity of the three cone types in the short, medium, and long areas of the spectrum (respectively, the portions of the spectrum corresponding to blue, green, and red).

Weighting a total spectral power distribution by the spectral sensitivities of the three kinds of cone cells gives three values of the stimulus; these three values compose a tristimulus specification of the perceived colour [41]. Each colour perceived by the human eye can be therefore described by a set of three coordinates, XYZ, derived for opaque or translucent media as follows:

$$X = \frac{K}{N} \int_\lambda S(\lambda) \cdot I(\lambda) \cdot \overline{x}(\lambda) \, d\lambda \tag{1}$$

$$Y = \frac{K}{N} \int_\lambda S(\lambda) \cdot I(\lambda) \cdot \overline{y}(\lambda) \, d\lambda \tag{2}$$

$$Z = \frac{K}{N} \int_\lambda S(\lambda) \cdot I(\lambda) \cdot \overline{z}(\lambda) \, d\lambda \tag{3}$$

where $\overline{x}(\lambda)$, $\overline{y}(\lambda)$, and $\overline{z}(\lambda)$ are the colour-matching functions, $S(\lambda)$ is the reflectance or the transmittance of the coloured surface, $I(\lambda)$ is the light source spectrum, N is the integral of the product $I(\lambda) \times \overline{y}(\lambda)$, and K is a normalisation factor, usually 1 or 100. This set of equations constitutes the link between the colour sensation derived by the human visual system, and the reflectance or transmittance of the medium illuminated by a given light source. By this set of equations, it is possible to calculate the tristimulus values, X, Y and Z, and thus to define the colour perceived by a standard observer. On the contrary, it is not possible to match the exact spectral transmittance or reflectance of an arbitrarily chosen colour from the tristimulus values, since there are only three types of cones to sample the entire visible spectrum. As a consequence, two different energy distributions can produce the same three cone signals so that the visual system perceives the same colour and those two energy distributions are said to be metamers [39].
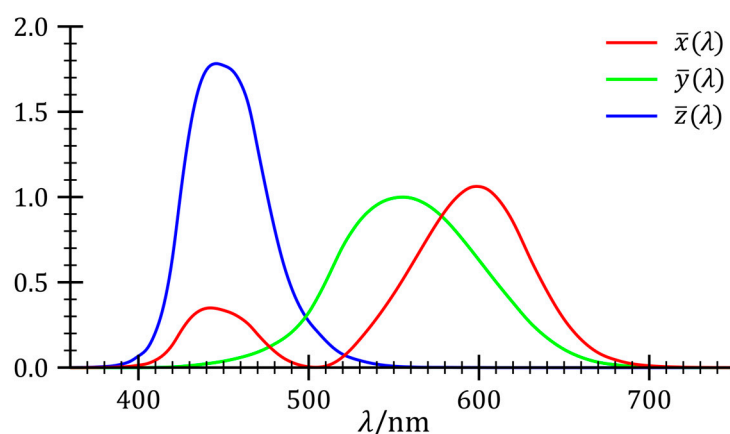
Figure 3. CIE colour matching functions 1932 2°. Reproduced with permission from [42], copyright 2007, Wiley.

4.2. Theoretical Optimal Features of Coloured BIPV Products

Some theoretical research has been carried out to determine the relationships between the colours of modules and their power losses. These studies estimated the coloured modules' efficiency by calculating the solar irradiance impinging on the PV cells as the product of $I(\lambda) \times (1 - R(\lambda))$, where $I(\lambda)$ is the irradiance spectrum of a light source, usually standard AM1.5 G or D65 illuminant, and $R(\lambda)$ is the spectral reflectance of the coloured layer, the same parameter responsible for the perceived colour [15].

Ideally, a coloured PV panel should reflect just a narrow portion of the visible spectrum while avoiding absorption effects and transmitting the remainder, so that the perceived colour is the one associated with a specific wavelength, while the rest of the spectrum can be absorbed by the cell and transformed into electricity.

Peharz et al. [16] quantified the theoretical power output of a crystalline silicon solar cell as a function of ideal monochromatic colour, generated by narrow pill box flat-top reflective spectra, centred in the short, medium, and long areas of the spectrum (corresponding to blue, green, and red), with wavelength span varying from 20 to 40 nm. To obtain the pill box spectra, the study used a classic RAL colour set and measured it with a two-beam spectrophotometer, equipped with an integrating sphere, to obtain the spectral reflectance of the colour in the wavelength interval between 300 and 1200 nm. The colour's reflectance in the visible spectrum was then used to calculate the sample's colour coordinates, by combining it with the colour-matching functions and the spectral power distribution of the D65/2° standard illuminant. The colours' coordinates have been set as the target of an algorithm that allowed generation of the pill box reflection spectra that matched the coordinates of the measured RAL colour (Figure 4). By combining the obtained spectral reflectance with the spectral power distribution of the light source and an ideal spectral response of a silicon solar cell, the authors calculated the photocurrent generated as a function of each specific colour and analysed the results in terms of relative power loss, in comparison to a reference device with zero reflection and maximum power conversion. The study highlighted significant differences in the power losses calculated using the monochromatic flat-top spectral band and the actual measured spectral reflectance, referred to the same opaque colour. The spectral reflectivity of a monochromatic colour is characterised by a narrow band higher than zero around the specific wavelength associated with the desired colour, while in the remaining solar spectrum, it is set to zero (Figure 4). This approach overlooks the possible reflections in the ultraviolet (UV) and near-infrared (NIR) portions of the spectrum, where solar cells are usually sensitive, leading to overestimation of a module's power output as four to five times higher than that associated with the measured reflection spectra. The study is merely theoretical since the optical features of coloured surfaces are a consequence of their chemical and physical properties, which are typical of a specific technology or material. Nonetheless, it provides useful information on the

required trade-off between colour perception and photovoltaic losses. By analysing the colour efficiency of each class of colours (defined as the ratio between the colour perception, given by the sum of the tristimulus values X, Y, and Z, and the difference between the reference photocurrent density (no reflection) and the photocurrent density derived from the reflection spectrum used to calculate the tristimulus values), the authors found that usually darker colours, around the wavelength of 450 nm, have the highest colour efficiency, while the colours around the wavelength of 700 nm have the lowest colour efficiency. This can be easily understood by looking at the spectral response of a c-Si cell, which has a minimum in the first section of the visible spectrum (300–400 nm) and increases regularly until reaching a maximum near 850 nm. This means that, to render a vivid colour with a dominant wavelength near 700 nm, a consistent portion of the radiation in that range should be reflected and made unavailable to power conversion in the region of maximum response of the solar cell.
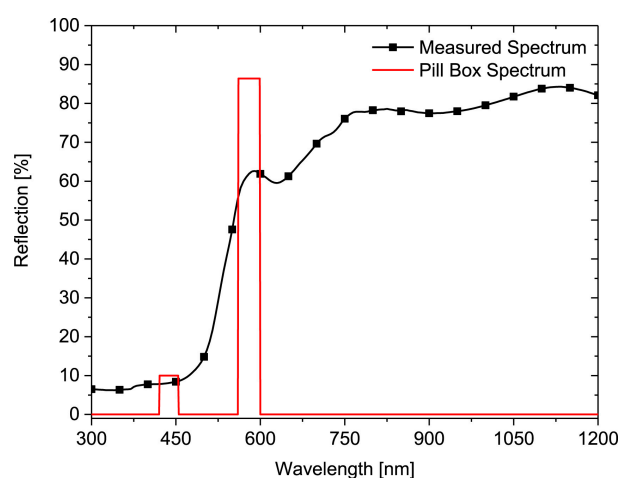

Figure 4. Example of the difference between measured and pill box reflection spectra of RAL colour 1004 "golden yellow". Reproduced with permission from [16], copyright 2018, Elsevier.

The work by Halme and Mäkinen [15], on the other hand, aimed at calculating the theoretical efficiency limit for opaque photovoltaics by assuming an ideal single-band-gap solar cell and neglecting the parasitic absorption losses and the possibility for multicarrier generation in the cell. The authors affirmed that this efficiency limit can be set as the upper limit for semi-transparent coloured cells as well. According to their investigation, the colour perception of the human eye is the only parameter to be considered to obtain an optimal colour, able to compromise efficiency and aesthetic by reflecting the lowest possible number of photons that would be used for electricity conversion in the cell. Following this principle, the reflection of wavelengths close to the peaks of the normalised colour-matching functions should be prioritised through sharp reflectance bands with a maximum value of R = 1 within the band and R = 0 elsewhere, to match the spectral sensibility of the human eye. By leveraging the colourimetry principle that any colour can be obtained through a linear combination of two monochromatic colours, the authors used two narrow reflection bands centred at the peak of the $\bar{z}/\lambda$ function at 444 nm and between the wavelengths 505 nm and 670, where the two functions $\bar{x}/\lambda$ and $\bar{y}/\lambda$ are predominant and the Z coordinate is not much affected. In this way, it was possible to produce all the achievable colours under the AM1.5G spectrum. Once the colour was obtained, the cell efficiency was optimised by calculating the best band gap energy E_g and the operating voltage V. The results were broken down by relative luminosity, i.e., the normalised Y coordinate of the CIE XYZ colour space, which can be used to represent the colour brightness, highlighting that almost the entire sRGB colour space can be obtained (Figure 5a) with an efficiency limit that ranges from 28% to 32%, with relative luminosity equal to Y = 0.25 (Figure 5b). Since to reproduce brighter colours a higher number of photons must be reflected, the relative luminosity

increases. Consequently, the efficiency limit decreases for colours with higher relative luminosity, ranging from 27% to 30% for Y = 0.50 and from 25% to 28% for Y = 0.75. The relative luminosity has a negative effect also on the short circuit current density, while it has a smaller effect on other electrical parameters (band gap energy, open-circuit voltage, and fill factor).
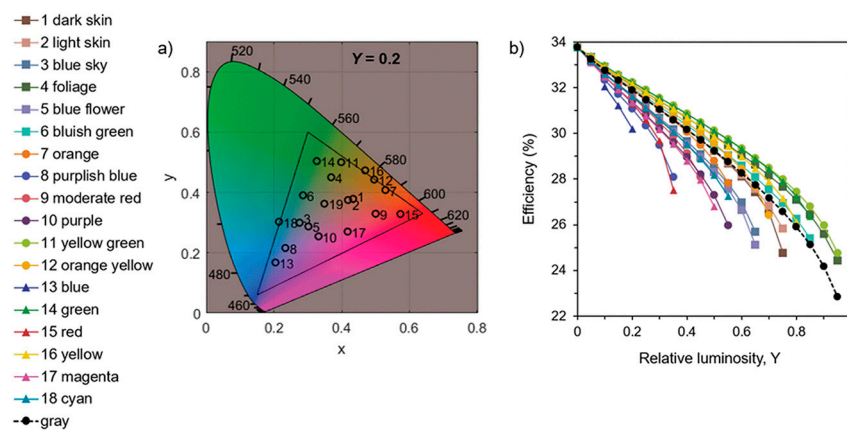

Figure 5. Effects of colour brightness (relative luminosity, *Y*) on the theoretical efficiency limits (subfigure (**b**)) for different colours, represented on the trichromatic chart in subfigure (**a**). Reproduced from ref. [15] with permission from the Royal Society of Chemistry.

The findings of these researchers differed in identifying the most efficient colours; Halme and Mäkinen [15] found that, when comparing colours with the same relative luminosity, the yellow-green colours were the most efficient, while the work from Peharz et al. [16] identified the blue and red colours as more efficient than green. As highlighted already by Røyset et al. [17], these differences might arise because Peharz et al. [16] compared colours with different relative luminosity. Therefore, starting from the consideration that only colours with the same relative luminosity, or lightness, can be compared in terms of colour efficiency, Røyset et al. [17] elaborated an alternative approach to determine efficiency losses in coloured BIPVs, by investigating not only flat-top reflectance spectra but also by modelling more realistic reflectance spectra that avoid sharp modifications for subsequent wavelengths, thus being more representative of a real reflectance curve measured from coloured BIPV samples. Indeed, as demonstrated by the authors, spectral reflectance measured on commercially available modules does not presents sharp and discontinuous flat-top reflectance, but rather continuous reflectance curves, quite diverse from ideal monochromatic colours. As a matter of fact, among advanced colour manufacturing techniques, narrow bandwidth reflectance, similar to the ideal flat-top high saturated monochromatic reflectance used in [15,16], is achievable by using guided-mode resonances (GMRs)-based colour filters [37]. On the other hand, colours realised with selective filters, multi-layered coating, and structural colours based on optical resonance thin-film structure, present smooth variations in the spectral optical properties, which makes the flat-top reflectance approach biased with overestimation of the real colour efficiency. This result was indeed already demonstrated by Peharz et al. [16] where the power losses related to colours obtained with monochromatic flat-top reflectance were compared to the ones related to measured colours from the RAL set. To generate more smoothly varying spectral features for target colours, Røyset et al. [17] introduced a sinusoidal function to generate wavelength reflectance transition for subsequent wavelengths. Five spectral reflectances were considered, which were centred at wavelengths 400, 450, 550, 600, and 700 nm; reflectance below λ_0 = 400 nm and above λ_4 = 700 nm was set at 4%, while the others could range between 4% and 80% and were generated by targeting the colour coordinate requirements (Figure 6). A transfer matrix was used to obtain a linear relationship between colour coordinates and spectral reflectance features, as well as between colour coordinates

and relative losses in the visible spectrum. The main drawback of generating more realistic spectral reflectance is that the achievable colour gamut is reduced. Nonetheless, by defining a colour performance index (CPI) as the ratio between the Y colour coordinate (which can be used as a figure of merit of the luminous reflectance factor, since the related colour matching function $\bar{y}(\lambda)$ is representative of the eye photopic sensitivity) and the relative power losses P, and referring to the CIE L*a*b* (where L* is the colour lightness, a* is the relative position of the colour between red and green, and b* is the relative position of the colour between blue and yellow) and L*C*h* (where L* is the colour lightness, C* is the colour chroma, and h* is the colour hue) colour spaces, the authors demonstrated that the lightness was the predominant parameter in the determination of the colour relative power losses, with a positive exponential correlation between the two parameters (Figure 7). The next predominant parameter was the hue. For colours in the medium lightness L* = 50 range (Y = 0.18), a minimum loss for green colour of 3.2% can be achievable, while the model predicted a relative loss varying from 9 to 16% for more realistic colours.
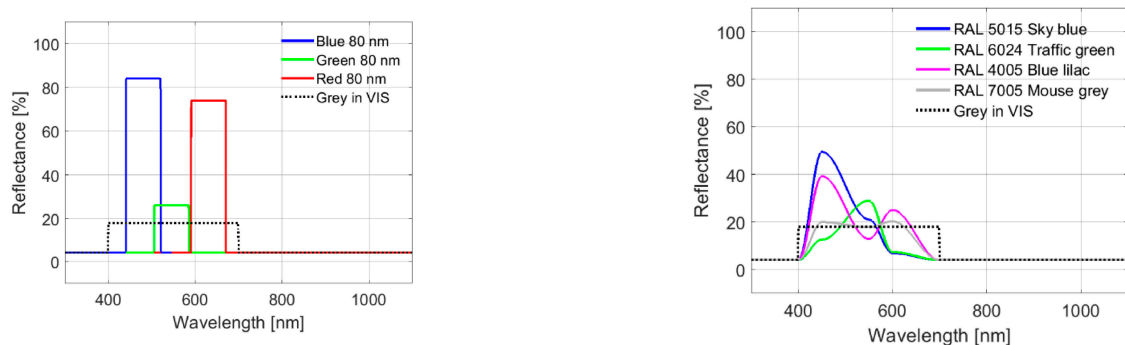

Figure 6. Example of reflectance spectra modelled by Røyset et al. [17]. On the left, the pill box monochromatic reflectance of blue, green, and red colours. On the right, smooth reflectance curves are generated by sinusoidal function wavelength transition, based on five main reflectance bands. Reproduced with permission from [17], copyright 2018, Elsevier.
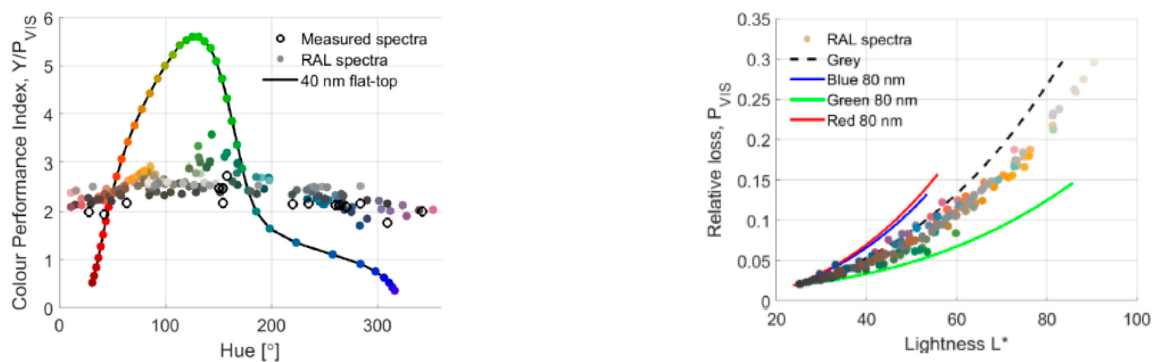

Figure 7. Colour performance index versus hue, and relative losses versus lightness, in the visible spectrum, as calculated by Røyset et al. [17]. Reproduced with permission from [17], copyright 2018, Elsevier.

A narrow pill-box reflectance spectrum was used also in the investigation by Li and Ma [43], who analysed the theoretic efficiency limit of coloured c-Si cell-based BIPV modules, with a five-parameter electrical model that took into account the current–voltage characteristic of the PV cell. The findings of this research agreed with the works previously analysed in this section and highlighted how brighter colours present lower efficiency and higher power losses, with an efficiency limit of 19.8% for pure white.

The above-mentioned research made use of theoretical approaches to investigate the ideal efficiency limits of coloured BIPVs. To do so, simplifications were used in both

the colour analysis/optimisation and the modelling of the electric features of PV cells. Nonetheless, these studies provide extensive information about optimal colour formation principles and clarify the role of the main colour parameters in the definition of the colour efficiency associated with the photovoltaic effect.

5. Modelling and Simulation to Optimise Coloured BIPV Performance

5.1. Modulation of the Anti-Reflective Coatings in Crystalline Silicon PV Cells

The deposition of anti-reflection coatings (ARCs) is a standard in c-Si cell manufacturing since it reduces the reflectance of the bare cell and improves the photon collection of the device and its power production. The most widely used technique to create ARCs is by depositing a thin layer of amorphous, hydrogenated silicon nitride a-SiNx:H through plasma-enhanced chemical vapour deposition (PECVD). This thin layer, besides improving the cell efficiency, contributes also to the definition of the cell's final colour since it has different optical constants with respect to the base c-Si cell [44]. In particular, modifying the thickness and refractive index of the ARCs, or adding multiple thin layers on the PV cell surface, affects the overall optical properties of the device; fine-tuning these two parameters leads to modification in the overall reflectance of the device, and thus, its colour [45]. The existing studies that aimed to investigate the relationship between the optical properties of deposited thin film and the colour of c-Si PV cells mainly exploited optical simulations to calculate the final total transmittance and reflectance of the cells. Usually, the former is used to assess the power generation, while the latter is used to define the colour, according to colourimetric principle (see Section 4.1).

J.H. Selj et al. [45] investigated single and multilayer film deposited by PECVD and multilayer ARCs produced with electrochemical etching of nanoporous silicon (PS). The optical modelling of the single and multiple layers was performed by using a pre-defined software package, while for the PS layer ellipsometry software was used. Before performing the simulations, single layers' thicknesses were measured at variable angles via an ellipsometer. Furthermore, reflectance measurements were performed by using an experimental design which included an integrating sphere. This study neglected the influence of encapsulation on the final colour rendering and PV efficiency, as well as shading losses and surface texture. Good approximation between the modelled and measured results was demonstrated.

Shen et al. and Minghua et al. [44,46], on the other hand, investigated in two studies the possible colour modulation of a PV cell with double-layer ARC (DARC) made by depositing a different thin layer on the standard SiNx:H layer by PECVD. The first study used ray tracing software to analyse the silicon cell texture, while the second simulated it by Monte Carlo ray tracing method. The optical features of the stack were investigated by varying the layers' thickness and refractive indices. According to their findings, colourful solar cells are obtained to the detriment of the generated photocurrent and efficiency. Nonetheless, using double ARCs improved the performance of a cell with a single ARC while guaranteeing flexibility in colour modulation, mainly for MgF$_2$ and SiO$_2$ top layers.

McIntosh et al. [47,48] improved the simulation approach by investigating the effect of encapsulation in addition to that of the ARC. They used a software-based advanced ray tracing, taking as input the thickness and refractive index of (i) the glass, (ii) the encapsulant (EVA), (iii) the ARC coating, and (iv) the c-Si bare cell. The presence of the encapsulant in close contact with the ARC induced a reduction in the reflectance in the first portion of the electromagnetic spectrum and an increase in wavelength from 400 to 900. This was to the detriment of the brightness of the perceived colour and the generated photocurrent (Figure 8).
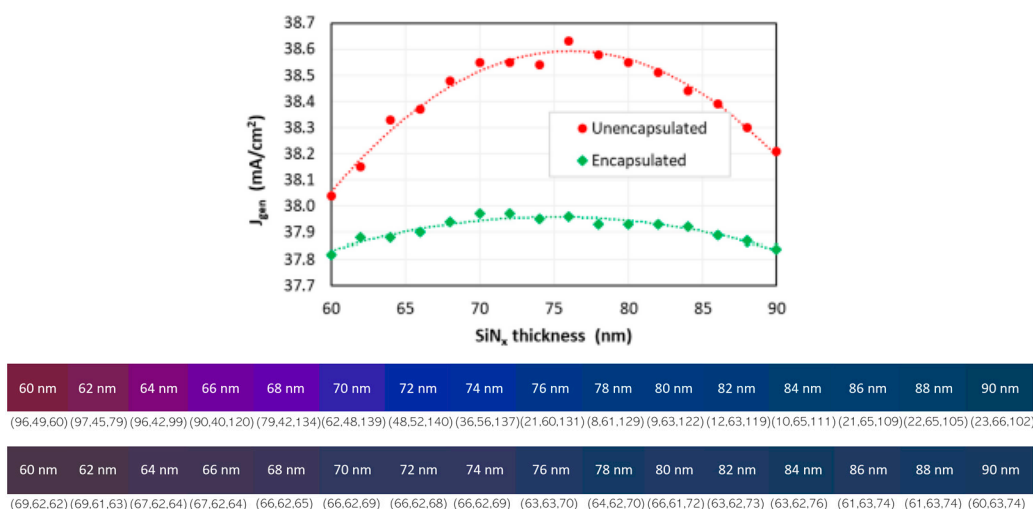
60 nm	62 nm	64 nm	66 nm	68 nm	70 nm	72 nm	74 nm	76 nm	78 nm	80 nm	82 nm	84 nm	86 nm	88 nm	90 nm
(96,49,60)	(97,45,79)	(96,42,99)	(90,40,120)	(79,42,134)	(62,48,139)	(48,52,140)	(36,56,137)	(21,60,131)	(8,61,129)	(9,63,122)	(12,63,119)	(10,65,111)	(21,65,109)	(22,65,105)	(23,66,102)

60 nm	62 nm	64 nm	66 nm	68 nm	70 nm	72 nm	74 nm	76 nm	78 nm	80 nm	82 nm	84 nm	86 nm	88 nm	90 nm
(69,62,62)	(69,61,63)	(67,62,64)	(67,62,64)	(66,62,65)	(66,62,69)	(66,62,68)	(66,62,69)	(63,63,70)	(64,62,70)	(66,61,72)	(63,62,73)	(63,62,76)	(61,63,74)	(61,63,74)	(60,63,74)

Figure 8. Generated photocurrent (**on the top**) and perceived colour (**on the bottom**) as a function of the SiNx thickness, before and after encapsulation. Reproduced with permission from [47], copyright 2018, AIP Publishing.

Amara et al. [49] used a similar simulation approach that took into account the layers' optical properties. In addition, the authors provided insight into the effect of colour on the cell temperature, showing that modification of the ARC thickness does not affect the efficiency much, and that this is partially due to a constant thermalisation level.

Furthermore, the study from Ortiz Lizcano et al. [50] used advanced ray tracing software to investigate the influence of colour on the electric and thermal behaviour of a crystalline silicon cell. The investigated colouring technique concerned the realisation of optical filters (OF), which are multilayer systems based on light interference. This technique allowed them to realise optical filters with high reflectance in a narrow wavelength range, by overlapping layers with the proper refractive index. The authors investigated the effect of the deposition of such a filter on the encapsulating glass of a PV module or on the c-Si cell. The simulation framework used was quite complex and employed a colour perception model to estimate the produced colour starting from a calculated reflectance curve. The authors developed both a spectrally resolved optical model and a two-dimensional finite volume transient thermal model. On this basis, the effect on the power conversion efficiency was then evaluated by deploying TCAD Sentaurus and a two-diode electrical model that considered angle-dependent modifying factors.

Yu et al. [51] achieved the goal of an efficient and colourful silicon-heterojunction structure by engineering the charge-selective contact layer on top of silicon cells. To fulfil the demand for highly conductive and controlled materials, Poly (3,4-ethylenedioxythiophene) polystyrene sulfonate (PEDOT:PSS) was employed for optical qualities in the charge-selective contact layer. The optimisation was performed by controlling either the thickness or the refractive index of the contact layer and using optical simulation to determine the device's spectral reflectance and colour perception.

From this overview, it is evident that the colour-tuning of crystalline silicon solar cells is usually obtained by modulating the thickness and optical properties of the ARC or the added deposited layers. The investigation of achievable colours and the influence on the electric parameter is usually performed by simulating the optical behaviour of the device and analysing the entire achievable colour gamut.

Conversely, optimisation algorithms for retrieving the layer composition for a target colour are scarce. In the end, these studies have demonstrated that the colour gamut achievable by using this colourisation technique is quite extended, even if the obtained solar cells usually appear metalised and iridescent.

5.2. Coloured Solar Glass for Opaque c-Si and CIGS PV Modules

One of the most diffused techniques to introduce colour in BIPV modules is the modification of the front glass in the modules' stack. The front glass can be coloured or digitally printed to mimic the appearance of traditional building materials or any other pattern or design. This method guarantees that the PV cells are invisible to the naked eye. The front glass may also be texturised to create a variety of finishes [31]. Although the numerous customisation possibilities provide significant architectural benefits, modification in the front glass causes changes in its optical behaviour, which may reflect or absorb a portion of the solar spectrum that would otherwise reach the PV cells and be utilised to generate power. Several studies provided experimental evidence of the effect that a printed glass has on the electric performance of the final module when it reproduces a specific colour [26,28,38,52,53]. However, to further develop such modules, the key issue to be addressed is to find the best balance of aesthetic and energy efficiency. Finding the optimal balance in this trade-off might provide high flexibility in the manufacturing of efficient products, which is a relevant characteristic to enhance the use of BIPV technology [18,23,54]. In recent years, some research has addressed this challenge, providing models able to predict the power output as a function of a target colour and/or a given print opacity. Saw et al. [55] explored regression analysis to link the print opacity and ink density to power output, exploiting experimental measurements conducted on six NCS colours digitally printed on low-iron tempered glass with no antireflection coating and with ceramic inks at different opacity ranging from 10% to 100%. Sixty total colour samples were produced and laminated on single-cell 20×20 cm minimodules using 5BB mono-PERC solar cells, EVA encapsulant, and black back sheet. The samples were analysed through I-V measurement at standard conditions. A reference module with uncoloured front glass was produced and analysed under the same test conditions to evaluate the relative performance of each colour and opacity. Regression modelling was performed on the tests' results using a statistical software to establish the relation between printing opacity and electric parameters of the laminated module. These results were used to predict the module electric performance for any printed opacity. This procedure led to the identification of a characteristic regression equation for each colour, ranging from linear correlation for the green to third-order polynomial correlation for the white. The error of the model in predicting the short circuit current associated with a colour for any given printing opacity was lower than 1%. The results showed that the effect of print opacity on the short circuit current and maximum generated power depends on the colour. The blue colour presented lower losses in terms of short circuit current and the maximum generated power, whereas the black presented the highest losses. Furthermore, the effect of colour and print opacity on the open circuit voltage and the fill factor of the mini modules was investigated. In general, open circuit voltage varies logarithmically with the short circuit current; therefore, the results showed that the black colour had the most evident variation, with open circuit voltage decreasing with increasing print opacity due to the high reflectivity of the colour also in the infrared region, which causes lower external quantum efficiency and generated short circuit current. The same behaviour was highlighted concerning the fill factor, which increased with print opacity and presented the highest values for the black. These results depended on the specific technology used to colour the glass, i.e., digital ceramic ink printing. Indeed, from external quantum efficiency measurements, the authors detected low transparency of some colour also in the infrared region. This behaviour was predominant for the black colour. The same study was later improved [56] by developing a model based on machine learning (ML) techniques. The updated model evaluated three different ML algorithms that aimed at predicting short circuit current for target colours in the RGB colour space, which was used to simulate the other electrical parameters based on the one-diode equation. The study also used the output of the ML model to predict the electric performance of multi-coloured BIPV modules.

Gasonoo et al. [54] and Kim et al. [57] used optical simulation software to optimise the manufacturing of coloured layers produced by multilayer deposition of titanium nitride

(TiN) and aluminium nitride (AlN) on the front glass and additive manufactured tri-dimensional optical patterns. Starting from tabulated information on the optical properties of each layer in the module's stack, the authors investigated the achievable colour gamut as well as the angular dependency of the spectral reflectance of the obtained colours. These results were used for the calculation of the PV module's electric performance. The authors demonstrated that the deposition of multiple alternated layers of titanium nitride (TiN) and aluminium nitride (AlN) on the front glass allows producing a quite large colour gamut while maximising the spectral transmittance of the coloured layer [54]. In [57], the authors demonstrated that additive-manufactured tri-dimensional optical patterns are more efficient in power conversion than a conventional colour layer for the same colour.

5.3. Coloured Additional Layers for Opaque c-Si and CIGS PV Modules

Gewohn et al. [20,58] used an experimental approach similar to Saw et al. [55] and based on measured external quantum efficiency and reflectance of modules coloured with eight colourants (CMYK, RGB, and white) to develop a model for the prediction of final appearance and yield of arbitrarily coloured BIPV modules. The model was based on coloured textile (CoTex) layers that were laminated onto the front glass. The model made use of colour vision theory to evaluate the final module's appearance using the halftone printing technique to render homogeneous colours. Halftone printing is based on three secondary inks, cyan (c), magenta (m), and yellow (y), which are printed in a dotted pattern rotated in relation to each other so that, from inks overlapping, mixed colours can be created (red (r), green (g), blue (b), and black (k)), whereas unprinted spots result in white colour. By using the Clapper–Yule model and the Fresnel equation, the proposed model calculated the reflectance of printed textile starting from the measured reflectance of printed modules with the three secondary colourants (Figure 9). All the generated colours were the result of the mix of the three secondary colourants, whose printing density could vary from 0% to 100%. The simulated colour was then evaluated against the printed colours through colour difference calculation. The calculation of the short-circuit current density was performed starting from the measured external quantum efficiency (EQE) of the modules printed with the three secondary inks. The optical model did consider internal reflection inside the printed textile and the reflectivity at the interface between the textile and the air. The results showed a good ability of the module in predicting the final target colour, with an average final colour difference for the 29 considered colours of 1.34, which means that the difference was barely perceptible to the human eye. The predicted short circuit current density showed a good deviation between calculated and measured values of 0.008. Furthermore, the study investigated the possible effect of printing inaccuracy, which is a fundamental aspect of colour replicability in printed PV modules. The accuracy in printing a target colour, evaluated with 26 variations, was marginal, with a maximum error of 3% in both colour difference and short circuit current density.
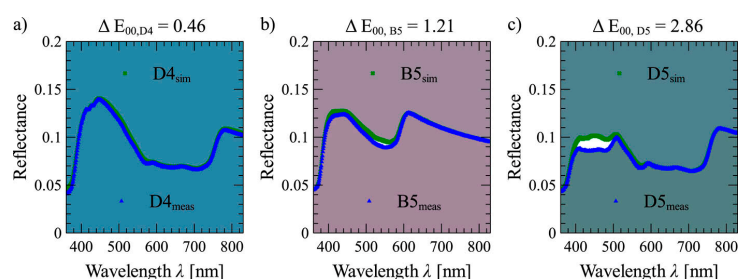

Figure 9. Examples of measured and simulated reflectance spectra for three target colours (D4 in subfigure (**a**), B5 in subfigure (**b**) and D5 in subfigure (**c**)) in the visible spectrum, and calculated colour difference. Reproduced with permission from [20], copyright 2021, AIP Publishing.

Slooff-Hoek et al. [21] developed two optical models to estimate the performance of coloured PV modules which were produced by laminating a digitally pixeled printed

interlayer between the front glass and the solar cells. The models made use of available colour conversion software to translate an image in RGB colour space into CYMK colour space upon printing. A defined absorption was assigned to each colour and each pixel by assuming (i) a linear dependence or (ii) a non-linear dependence of the transmission of each pixel and absorption of an individual colour. Furthermore, a fixed reflectance of the front side of the glass had been set at 4%. The models' parameters were determined by fitting the model to current-voltage test results on a single-cell and single-coloured laminate.

In the end, the non-linear model was validated on four patterns. The model was also used to adjust printing parameters to avoid mismatches between the module's strings.

6. Discussions

The existing models have used either optical parameters such as refractive index and extinction coefficient to run detailed optical simulations, or measured reflectance and external quantum efficiency of a laminated coloured BIPV module to develop models able to predict the aesthetic and performance of coloured modules.

The analysed research can be divided into two main categories: (i) the studies which propose theoretical approaches and models for assessing ideal features and efficiency limits of coloured layers in BIPVs, and (ii) the studies which propose modelling and/or simulations to optimise coloured BIPV performance for specific colouring techniques and PV technologies. The relevance of the first group of studies relies on the extensive awareness that they bring on the optimal colour formation principles for BIPV application, and in the clarification of the role of the main colour parameters in the definition of the colour efficiency associated with the photovoltaic effect. Nonetheless, the researchers do not provide insights on the challenges to be faced in translating those ideal optimal features in real coloured BIPV modules, and how the peculiarity of a specific manufacturing process could affect the energy conversion of a specific target colour. Instead, it is the second group of studies that expands our knowledge on these aspects, which is crucial to exploit the findings of the theoretical studies. Two main approaches have been used in this second group of studies to investigate the effect of coloured layers: (i) detailed optical modelling of the layers in the module's stack, including coloured layer, by using ray tracing techniques or Fresnel equations, and (ii) mathematical elaboration of the measured characteristics of the final product through different techniques (regression analysis, machine learning, fitting models). The main characteristics of the analysed studies have been summarised in Table 2. Following the categorisation proposed in Table 1, the studies have been broken down by colour layer position, colouring technique, colour layer typology, PV technology (if applicable), and colour layer appearance. For each category, the main inputs and outputs of the proposed models have been highlighted, as well as the specific modelling strategy used for the coloured layers.

Table 2. Overview of the main characteristics of the analysed studies broken down by colour layer position, colouring technique, colour layer typology, PV technology (if applicable), and colour layer appearance. For each category, the main input and output of the proposed models have been reported, as well as the specific modelling strategy used for modelling the coloured layers and the reference of the works.

Coloured Layer Position	Colouring Technique	Colour Layer Typology	PV Technology	Colour Layer Appearance	Model Input	Coloured Layer Modelling Strategy	Model Output	Ref.
Ideal coloured layer	n/a	n/a	c-SI	Continuous/monochromatic	Measured colour's reflectance spectra Spectral response of a c-SI cell Spectral power distribution of the light source	Narrow pill box flat-top reflective spectra	Generated photocurrent, relative power loss for RAL colours	[16]
						Linear combination of two monochromatic narrow reflection bands centred at the peak of the $\bar{z}/\lambda$ and between the two functions $\bar{x}/\lambda$ and $\bar{y}/\lambda$	Band gap energy (Eg), operating voltage (V), theoretical efficiency limit	[15]
						Sinusoidal function wavelength transition, based on five main reflectance bands	Efficiency losses Colour performance index (CPI)	[17]
Integrated (or embedded)	Modulation of the passivation coating or ARC thickness and/or refraction index	Coloured/coated active layer	c-SI	Continuous/monochromatic	Measured layers' thicknesses at variable angles Measured layers' optical constants	Optical modelling with predefined software package	Efficiency	[45]
					Measured layers' thicknesses at variable angles Measured layers' optical constants	Ray tracing software Monte Carlo ray tracing method	Generated photocurrent Efficiency	[44,46]
					Measured layers' thicknesses at variable angles Measured layers' optical constants (included encapsulant and front glass)	Ray tracing software Monte Carlo ray tracing method	Generated photocurrent Efficiency Colour of the encapsulated cell	[47–51]

Table 2. *Cont.*

Coloured Layer Position	Colouring Technique	Colour Layer Typology	PV Technology	Colour Layer Appearance	Model Input		Coloured Layer Modelling Strategy	Model Output	Ref.
Added (additional layer)	Ceramic printing of the front glass	Coated on front glass	c-SI	Continuous/monochromatic	Print opacity IV curves at STC		Regression analysis to link print opacity and electric output	Electric output for a specific NCS colour	[55]
				Continuous/discrete Monochromatic/ multi-coloured	Print opacity IV curves at STC		Machine learning techniques	Short circuit current for target colour	[56]
	Additional coloured/printed layer	Laminated on the front glass	c-SI	Continuous/monochromatic	Measured external quantum efficiency Measured reflectance of coloured modules		Halftone printing technique based on CMY colours, Clapper–Yule model, and Fresnel equation Reflectance of printed textile	Short circuit current density	[20,58]
		Deposited on the front glass			Tabulated optical properties of module's layers		Optical simulation with existing software	Achievable colour gamut Electric parameters	[54,57]
		Coloured polymeric interlayer		Continuous/monochromatic and pattern	Current–voltage test results on single cell single-coloured laminate Digital RGB image		Optical model based on fitting process to IV measurements	Electric parameters of full-coloured patterned PV modules	[21]

Measuring the spectral reflectance or the external quantum efficiency of a printed module could lead to undesired inaccuracy for the proposed models, since, for example, the back reflectivity at the interface between coloured layers and glass or encapsulant is neglected or considered multiple times. On the other hand, using optical parameters to run simulations, usually based on the transfer matrix method, is an accurate and flexible approach which enables different optimisation strategies. Nonetheless, measuring or deriving all the spectral properties of the involved material could be a tricky procedure that requires sophisticated instruments and highly specialised control of the production process. For example, measuring the optical parameters of the inks used for digital printing is difficult, since the test sample cannot be produced for the bare inks, which instead must be deposited on a substrate. Indeed, isolating the optical properties of coloured thin films from their substrate, or accounting for the optical coupling of the coloured layer with encapsulants, is not trivial. In this regard, the work of Kutter et al. [59] proposed a model to determine the actual spectral transmittance of a ceramic printed glass from simple spectrophotometry of the component taken in air. The model allowed correction of the measured transmittance in the air by considering the difference in refractive index between air and encapsulant (EVA), which determines a reduction in the reflectivity of the rear surface, resulting in higher transmittance of the encapsulated component. The study demonstrated a good accuracy of the model in predicting the transmittance of the encapsulated coloured glass and the relative module power, with a root-mean-square deviation (RMSE) of 0.73%, for a cover ratio ranging from 0% to 98%. However, Pfau et al. [60] have proposed a new experimental approach for the optical characterisation of ceramic inks to be used for digital printing. The method consists in measuring the reflectance of the samples after deposition on a special spectral broadband absorbed foil, which allows excluding the effect of the back reflectivity at the interface between the inks and the substrate. This experimental approach results in better accuracy of the proposed colour model, which uses the spectral optical characterisation of the inks and module internal quantum efficiency to run a simulation based on subtractive colour synthesis and CMYK+W colour model. The model evaluates the effect of the coloured layer on short circuit current density.

7. Conclusions

This paper investigated the available literature on models and techniques used for assessing the influence of coloured layers on power generation in customised opaque BIPV products. The analysis focused on models for opaque coloured BIPV modules, with coloured layers either embedded in the active components or included as additional layers in the module's stack. The ability to link colour and power generation is considered a key step in helping to reduce the cost of coloured BIPV products, by easing mass manufacturing while preserving the customisation potential and, therefore, enhancing their market uptake in the construction sector. Indeed, having greater control over the production process, and being able to assess in advance the influence of the coloured layers on the module's power generation, would avoid the need for prototyping, thereby allowing for optimisation of the product performance by reducing the time and costs of customised manufacturing. The findings of theoretical studies are crucial to expand our knowledge about optimal colour formation principles and the role of the main colour parameters in the definition of the colour efficiency associated with the photovoltaic effect. The studies which have proposed modelling and/or simulations for coloured BIPV performance optimisation, on the other hand, exploit the findings of the theoretical studies in real technologies, and they have the potential to improve dramatically the quality of the mass customisation of coloured products. The two approaches used in this research have both benefits and shortcomings. Using optical models of the coloured layers, ray tracing techniques, or Fresnel equations and transfer matrix methods, offers a high level of accuracy and flexibility in defining the optimisation strategies. Nonetheless, this approach requires the detailed optical characterisation of each layer in the module's stack and of each coloured layer, to be used as input

data for the model. This activity can be complex and might require sophisticated equipment and high control for the experimental set-up. Whereas experimental approaches based on measurements of the electric output of the coloured BIPV module offer advantages in model data acquisition, they could suffer from an undesirable inaccuracy due to underestimation of the interreflections among the module's layers. Furthermore, initial data acquisition must be repeated after each modification of the manufacturing process or of the coloured layer characteristics. In the future, the combination of the described approaches can provide more accurate and flexible models. In particular, the flexibility of detailed optical models should be exploited by using input data obtained with simpler equipment and procedures. Furthermore, future models should consider the effect of coloured layers on the module's temperature and the influence of different incident angles for the solar radiation on both aesthetic and energy performance. This would give BIPV manufacturers useful tools for implementing mass customisation of BIPV modules while ensuring flexibility in the design, improvement of the manufacturing techniques, and reliability of the final products.

References

1. Lovati, M.; Salvalai, G.; Fratus, G.; Maturi, L.; Albatici, R.; Moser, D. New method for the early design of BIPV with electric storage: A case study in northern Italy. *Sustain. Cities Soc.* **2019**, *48*, 101400. [CrossRef]
2. Chen, S.; Yao, H.; Hu, B.; Zhang, G.; Arunagiri, L.; Ma, L.-K.; Huang, J.; Zhang, J.; Zhu, Z.; Bai, F.; et al. A Nonfullerene Semitransparent Tandem Organic Solar Cell with 10.5% Power Conversion Efficiency. *Adv. Energy Mater.* **2018**, *8*, 1800529. [CrossRef]
3. IEA. PVPS Task 15 Subtask E. In *Report T15-07—Coloured BIPV Market, Research and Development*; IEA: Paris, France, 2019.
4. Causone, F.; Scoccia, R.; Pelle, M.; Colombo, P.; Motta, M.; Ferroni, S. Neighborhood Energy Modeling and Monitoring: A Case Study. *Energies* **2021**, *14*, 3716. [CrossRef]
5. Causone, F.; Tatti, A.; Alongi, A. From Nearly Zero Energy to Carbon-Neutral: Case Study of a Hospitality Building. *Appl. Sci.* **2021**, *11*, 10148. [CrossRef]
6. Petter Jelle, B.; Breivik, C.; Drolsum Røkenes, H. Building integrated photovoltaic products: A state-of-the-art review and future research opportunities. *Sol. Energy Mater. Sol. Cells* **2012**, *100*, 69–96. [CrossRef]
7. Di Bella, A.; Canti, F.; Prina, M.G.; Casalicchio, V.; Manzolini, G.; Sparber, W. Multi-Objective Optimization to Identify Carbon Neutrality Scenarios for the Italian Electric System. *SSRN Electron. J.* **2022**. Available online: https://ssrn.com/abstract=4134221 (accessed on 22 January 2023).
8. Heinstein, P.; Ballif, C.; Perret-Aebi, L.-E. Building Integrated Photovoltaics (BIPV): Review, potentials, barriers and myths. *Green* **2013**, *3*, 125–156. [CrossRef]
9. Saretta, E.; Bonomo, P.; Frontini, F. Active BIPV Glass Facades: Current Trends of Innovation. In Proceedings of the GPD Glass Performance Days 2017, Tampere, Finland, 28–30 June 2017.
10. Freitas, S.; Brito, M.C. Solar façades for future cities. *Renew. Energy Focus* **2019**, *31*, 73–79. [CrossRef]
11. Scognamiglio, A.; Berni, F.; Frontini, C.S.P.L.; Maturi, L. The Complex Dialogue between Photovoltaics and Pre-Existing: Starting Point for a Discussion. In Proceedings of the 27th European Photovoltaic Solar Energy Conference and Exhibition, Frankfurt, Germany, 24–28 September 2012; pp. 4161–4168.

12. Escarre, J.; Li, H.Y.; Sansonnens, L.; Galliano, F.; Cattaneo, G.; Heinstein, P.; Nicolay, S.; Bailat, J.; Eberhard, S.; Ballif, C.; et al. When PV modules are becoming real building elements: White Solar Module, a Revolution for BIPV. In Proceedings of the 2015 IEEE 42nd Photovoltaic Specialist Conference PVSC, New Orleans, NO, USA, 14–15 June 2015; pp. 1–2.
13. Xiang, C.; Matusiak, B.S.; Røyset, A.; Kolås, T. Pixelization approach for façade integrated coloured photovoltaics-with architectural proposals in city context of Trondheim, Norway. *Sol. Energy* **2021**, *224*, 1222–1246. [CrossRef]
14. Lee, H.; Song, H.J. Current status and perspective of colored photovoltaic modules. *Wiley Interdiscip. Rev. Energy Environ.* **2021**, *10*, e403. [CrossRef]
15. Halme, J.; Mäkinen, P. Theoretical efficiency limits of ideal coloured opaque photovoltaics. *Energy Environ. Sci.* **2019**, *12*, 1274–1285. [CrossRef]
16. Peharz, G.; Ulm, A. Quantifying the influence of colors on the performance of c-Si photovoltaic devices. *Renew. Energy* **2018**, *129*, 299–308. [CrossRef]
17. Røyset, A.; Kolås, T.; Jelle, B.P. Coloured building integrated photovoltaics: Influence on energy efficiency. *Energy Build.* **2020**, *208*, 109623. [CrossRef]
18. Pelle, M.; Canosci, E.; Luzi, G.; Maturi, L. Hidden colored Building Integrated Photovoltaics: Technology overview and design challenges. In Proceedings of the International Conference on Solar Energy for Buildings and Industry, Kassel, Germany, 25–29 September 2022.
19. Forberich, K.; Guo, F.; Bronnbauer, C.; Brabec, C.J. Efficiency Limits and Color of Semitransparent Organic Solar Cells for Application in Building-Integrated Photovoltaics. *Energy Technol.* **2015**, *3*, 1051–1058. [CrossRef]
20. Gewohn, T.; Schinke, C.; Lim, B.; Brendel, R. Predicting color and short-circuit current of colored BIPV modules. *AIP Adv.* **2021**, *11*, 095104. [CrossRef]
21. Slooff-Hoek, L.H.; van Strien, W.; Sepers, T.; Gijzen, G.; Minderhoud, T.; Carr, A.J.; Burgers, A.R.T. Model to Estimate the Performance of Full-Colored Solar Panels. In Proceedings of the 8th World Conference on Photovoltaic Energy Conversion, Milano, Italy, 26–30 September 2022; pp. 512–516.
22. Palm, J.; Tautenhahn, L.; Weick, J.; Kalio, R.; Kullmann, J.; Heiland, A.; Grinsteid, S.; Schmidt, N.; Borowski, P.; Karg, F. BIPV Modules: Critical Requirements and Customization in Manufacturing. In Proceedings of the 2018 IEEE 7th World Conference on Photovoltaic Energy Conversion, WCPEC 2018—A Joint Conference of 45th IEEE PVSC, 28th PVSEC & 34th EU PVSEC, Waikoloa, HI, USA, 10–15 June 2018; pp. 2561–2566.
23. Pelle, M.; Lucchi, E.; Maturi, L.; Astigarraga, A.; Causone, F. Coloured BIPV Technologies: Methodological and Experimental Assessment for Architecturally Sensitive Areas. *Energies* **2020**, *13*, 4506. [CrossRef]
24. Roverso, R.; Pelle, M.; Dallapiccola, M.; Astigarraga, A.; Lucchi, E.; Ingenhoven, P.C.; Maturi, L. Experimental Assessment and Data Analysis of Colored Photovoltaic in the Field of BIPV Technology Application. In Proceedings of the 38th European Photovoltaic Solar Energy Conference and Exhibition, Online, 6–10 September 2021.
25. Maturi, L.; Belluardo, G.; Moser, D.; Del, M. BiPV system performance and efficiency drops: Overview on PV module temperature conditions of different module types. *Energy Procedia* **2014**, *48*, 1311–1319. [CrossRef]
26. Wittkopf, S. Building integrated photovoltaic at NEST—Preliminary test bedding results. *J. Phys. Conf. Ser.* **2019**, *1343*, 012090. [CrossRef]
27. Gewohn, T.; Koopmeiners, M.; Vogt, M.R.; Lim, B.; Schinke, C.; Brendel, R. Outdoor Testing Facility for an Experimental Validation of Yield Predictions. In Proceedings of the 37th European Photovoltaic Solar Energy Conference (EUPVSEC), Online, 7–11 September 2020; pp. 1915–1919.
28. Frontini, F.; Bonomo, P.; Saretta, E.; Weber, T.; Berghold, J. Indoor and Outdoor Characterization of Innovative Colored BIPV Modules for Façade Application. In Proceedings of the 32nd European Photovoltaic Solar Energy Conference and Exhibition, WIP, Munich, Germany, 20–24 June 2016; pp. 2498–2502.
29. Li, Z.; Ma, T.; Yang, H.; Lu, L.; Wang, R. Transparent and Colored Solar Photovoltaics for Building Integration. *Sol. RRL* **2021**, *5*, 200061. [CrossRef]
30. Tai, Q.; Yan, F. Emerging Semitransparent Solar Cells: Materials and Device Design. *Adv. Mater.* **2017**, *29*, 1700192. [CrossRef]
31. Grobe, L.O.; Terwilliger, M.; Wittkopf, S. Designing the Colour, Pattern and Specularity of Building Integrated Photovoltaics. In Proceedings of the ATI 2020: Smart Buildings, Smart Cities, Izmir, Turkey, 28–30 April 2020; pp. 44–53.
32. Ballif, C.; Perret-Aebi, L.-E.; Lufkin, S.; Rey, E. Integrated thinking for photovoltaics in buildings. *Nat. Energy* **2018**, *3*, 438–442. [CrossRef]
33. Institute, B.S. *BSI Standards Publication Glass in Building—Determination of Luminous and Solar Characteristics of Glazing*; AFNOR: Saint-Denis, France, 2011.
34. Eder, G.; Peharz, G.; Trattnig, R.; Bonomo, P.; Saretta, E.; Frontini, F.; Polo López, C.S.; Rose Wilson, H.; Eisenlohr, J.; Martin Chivelet, N.; et al. *Coloured BIPV-Market, Research and Development*; DIVA: Uppsala, Sweden, 2019; p. 60.
35. Kuhn, T.E.; Erban, C.; Heinrich, M.; Eisenlohr, J.; Ensslen, F.; Neuhaus, D.H. Review of technological design options for building integrated photovoltaics (BIPV). *Energy Build.* **2021**, *231*, 110381. [CrossRef]
36. Pascual-San José, E.; Sánchez-Díaz, A.; Stella, M.; Martínez-Ferrero, E.; Alonso, M.I.; Campoy-Quiles, M. Comparing the potential of different strategies for colour tuning in thin film photovoltaic technologies. *Sci. Technol. Adv. Mater.* **2018**, *19*, 823–835. [CrossRef]

37. Ji, C.; Lee, K.-T.; Xu, T.; Zhou, J.; Park, H.J.; Guo, L.J. Engineering Light at the Nanoscale: Structural Color Filters and Broadband Perfect Absorbers. *Adv. Opt. Mater.* **2017**, *5*, 170036. [CrossRef]
38. Ji, C.; Zhang, Z.; Masuda, T.; Kudo, Y.; Guo, L.J. Vivid-colored silicon solar panels with high efficiency and non-iridescent appearance. *Nanoscale Horiz.* **2019**, *4*, 874–880. [CrossRef]
39. Haase, C.S.; Meyer, G.W. Modeling pigmented materials for realistic image synthesis. *ACM Trans. Graph.* **1992**, *11*, 305–335. [CrossRef]
40. Carter, E.C.; Schanda, J.D.; Hirschler, R.; Jost, S.; Luo, M.R.; Melgosa, M.; Ohno, Y.; Pointer, M.R.; Rich, D.C.; Vienot, F.; et al. *CIE 015:2018 Colorimetry*, 4th ed.; CIE: Vienna, Austria, 2018.
41. Commission Internationale de L'Eclairage. Create colour model inspired by cones spectral sensitivity in the retina of the human eye. In Proceedings of the 4th CIE Expert Symposium on Colour and Visual Appearance, Prague, Czech Republic, 6–7 September 2016.
42. Schanda, J. *Colorimetry: Understanding the CIE System*; Wiley: Hoboken, NJ, USA, 2007.
43. Li, Z.; Ma, T. Theoretic efficiency limit and design criteria of solar photovoltaics with high visual perceptibility. *Appl. Energy* **2022**, *324*, 119761. [CrossRef]
44. Shen, H.; Altermatt, P.P.; Feng, Z.; Yang, Y.; Chen, Y. Color Modulation of c-Si Solar Cells without Significant Current-Loss by Means of a Double-Layer Anti-Reflective Coating. In Proceedings of the 27th European Photovoltaic Solar Energy Conference and Exhibition, Frankfurt, Germany, 24–28 September 2012; pp. 2014–2016.
45. Selj, J.H.; Mongstad, T.T.; Søndenå, R.; Marstein, E.S. Reduction of optical losses in colored solar cells with multilayer antireflection coatings. *Sol. Energy Mater. Sol. Cells* **2011**, *95*, 2576–2582. [CrossRef]
46. Li, M.; Zeng, L.; Chen, Y.; Zhuang, L.; Wang, X.; Shen, H. Realization of Colored Multicrystalline Silicon Solar Cells with SiO_2/SiN_x:H Double Layer Antireflection Coatings. *Int. J. Photoenergy* **2013**, *2013*, 352473. [CrossRef]
47. McIntosh, K.R.; Amara, M.; Mandorlo, F.; Abbott, M.D.; Sudbury, B.A. Advanced simulation of a PV module's color. *AIP Conf. Proc.* **2018**, *1999*, 020017.
48. McIntosh, K.R.; Cotsell, J.N.; Cumpston, J.S.; Norris, A.W.; Powell, N.E.; Ketola, B.M. An optical comparison of silicone and EVA encapsulants for conventional silicon PV modules: A ray-tracing study. In Proceedings of the 2009 34th IEEE Photovoltaic Specialists Conference (PVSC), Philadelphia, PA, USA, 7–12 June 2009; pp. 544–549.
49. Amara, M.; Mandorlo, F.; Couderc, R.; Gerenton, F.; Lemiti, M. Temperature and color management of silicon solar cells for building integrated photovoltaic. *EPJ Photovolt.* **2018**, *9*, 1. [CrossRef]
50. Ortiz Lizcano, J.C.; Procel, P.; Calcabrini, A.; Yang, G.; Ingenito, A.; Santbergen, R.; Zeman, M.; Isabella, O. Colored optic filters on c-Si IBC solar cells for building integrated photovoltaic applications. *Prog. Photovolt. Res. Appl.* **2022**, *30*, 401–435. [CrossRef]
51. Yu, L.M.; Man, J.X.; Chen, T.; Luo, D.; Wang, J.; Yang, H.; Zhao, Y.B.; Wang, H.; Yang, Y.; Lu, Z.H. Colorful conducting polymers for vivid solar panels. *Nano Energy* **2021**, *85*, 105937. [CrossRef]
52. Tzikas, C.; Valckenborg, R.M.E.; Dörenkämper, M.; van den Donker, M.; Lozano, D.D.; Bognár, Á.; Loonen, R.; Hensen, J.; Folkerts, W. Outdoor characterization of colored and textured prototype PV facade elements. In Proceedings of the 35th European Photovoltaic Solar Energy Conference and Exhibition, Brussels, Belgium, 24–28 September 2018.
53. Riedel, B.; Messaoudi, P.; Assoa, Y.B.; Thony, P.; Hammoud, R.; Perret-Aebi, L.-E.; Tsanakas, J.A. Color coated glazing for next generation BIPV: Performance vs aesthetics. *EPJ Photovolt.* **2021**, *12*, 11. [CrossRef]
54. Gasonoo, A.; Ahn, H.-S.; Lim, S.; Lee, J.-H.; Choi, Y. Color Glass by Layered Nitride Films for Building Integrated Photovoltaic (BIPV) System. *Crystals* **2021**, *11*, 281. [CrossRef]
55. Saw, M.H.; Singh, J.P.; Wang, Y.; Birgersson, K.E.; Khoo, Y.S. Electrical Performance Study of Colored c-Si Building-Integrated PV Modules. *IEEE J. Photovolt.* **2020**, *10*, 1027–1034. [CrossRef]
56. Saw, M.H.; Pravettoni, M.; Birgersson, E. STC Short-Circuit Current Prediction and I–V Simulation of Colored BIPV Modules With Machine Learning and One-Diode Equivalent Circuit Models. *IEEE J. Photovolt.* **2022**, *12*, 1533–1542. [CrossRef]
57. Kim, Y.-S.; Kim, A.-R.; Tark, S.-J. Building-Integrated Photovoltaic Modules Using Additive-Manufactured Optical Pattern. *Energies* **2022**, *15*, 1288. [CrossRef]
58. Gewohn, T.; Vogt, M.R.; Lim, B.; Schinke, C.; Brendel, R. Postproduction Coloring of Photovoltaic Modules With Imprinted Textiles. *IEEE J. Photovolt.* **2021**, *11*, 138–143. [CrossRef]
59. Kutter, C.; Wilson, H.R.; Pfreundt, A.; Heinrich, M.; Wirth, H. Light attenuation MODEL to predict nominal power of modules. In Proceedings of the 35th European Photovoltaic Solar Energy Conference and Exhibition, Brussels, Belgium, 24–28 September 2018.
60. Pfau, C.; Bangash, A.R.; Hagendorf, C.; Turek, M. Simulation Tool for the Performance Optimization of Colored PV Modules. In Proceedings of the 38th European Photovoltaic Solar Energy Conference and Exhibition, Online, 6–10 September 2021; pp. 769–772.